

# Catalytic and Non-catalytic Conversion of Methane to C<sub>2</sub> Hydrocarbons in a Low Temperature Plasma

Hamid Reza Bozorgzadeh

Research Institute of Petroleum Industry, West Blvd. of Azadi Sports Complex, Tehran, Iran

## ABSTRACT

The direct conversion of methane to C<sub>2</sub> hydrocarbons, in a quartz tube reactor enforced by a DC corona discharge, was investigated at atmospheric pressure. The process was carried out in the presence of metal oxide catalysts of Mn/W/SiO<sub>2</sub>, Mn/W/SiO<sub>2</sub> (tetraethyl orthosilicate, TEOS), and Mn/W/CNT (supported on carbon nanotubes). The total yield to C<sub>2</sub> hydrocarbons in the presence of metal oxide catalysts in plasma environment was in the order of Mn/W/SiO<sub>2</sub>> Mn/W/SiO<sub>2</sub> / TEOS> Plasma only> Mn/W/CNT. The order changes to Mn/W/SiO<sub>2</sub>>Mn/W/CNT>Plasma only> Mn/W/SiO<sub>2</sub>/TEOS, when the selectivity and yield of ethylene is considered. The highest yield to C<sub>2</sub> hydrocarbons was 15.8%, which was obtained by using Mn/W/SiO<sub>2</sub> in combination with gas discharge plasma without external heating; it was lower when the same feed composition was tested over this catalyst at 825 °C. The catalyst Na<sub>2</sub>WO<sub>4</sub>/Mn<sub>2</sub>O<sub>3</sub>/SiO<sub>2</sub>-b1, which produces the least carbon oxides, gives rise to the highest production of higher hydrocarbons and ethylene. Catalysts Na<sub>2</sub>WO<sub>4</sub>/Mn<sub>2</sub>O<sub>3</sub>/SiO<sub>2</sub> /TEOS-b2 and Na<sub>2</sub>WO<sub>4</sub>/Mn<sub>2</sub>O<sub>3</sub>/CNT-b3, due to their high selectivity toward carbon oxides, show low efficiency in producing more valuable hydrocarbons.

**Keywords:** Methane Conversion, Non-thermal Plasma, Catalysis, Metal Oxide, Hydrocarbons

## INTRODUCTION

Although methane is an excellent raw material for the production of fuels and chemicals, its main use is still restricted to fuel for power generation for domestic and industrial use. In many respects, methane is an ideal fuel for these purposes because of its availability in most populated centres, its ease of purification to remove sulphur compounds, and the fact that among the hydrocarbons, it has the largest heat of combustion relative to the amount of CO<sub>2</sub> formed. On the other hand, methane is a greatly underutilized resource for chemicals and liquid

fuels [1]. Methane can be converted directly to C<sub>2</sub> hydrocarbons by pyrolysis or thermal coupling. The reaction is highly endothermic and the heat must be supplied at high temperatures. Ethane, ethylene, benzene, and hydrogen are the main products. Excessive carbon formation can be avoided using short reaction times and low partial pressures of methane preferably by hydrogen dilution of the feed. More than 90% selectivity of C<sub>2</sub> hydrocarbons may be obtained from methane. High yields of ethane (>85%) are obtainable at extreme conditions of temperatures (> 2000 K) and short reaction times (<10<sup>-2</sup> s) [2, 3].

Methane can be converted to chemicals and

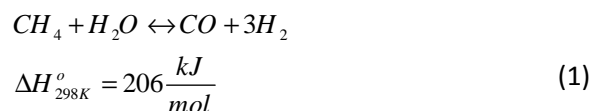
### \*Corresponding author

Hamid Reza Bozorgzadeh  
Email: bozorgzadehhr@ripi.ir  
Tel: +98 21 4473 9551  
Fax: +98 21 4473 9716

### Article history

Received: September 28, 2013  
Received in revised form: January 13, 2014  
Accepted: February 09, 2014  
Available online: February 20, 2015

fuels in two ways, either via synthesis gas or directly into C<sub>2</sub> hydrocarbons or methanol. Almost all commercial processes for large scale natural gas conversion involve synthesis gas. Steam reforming is the dominant process for the production of synthesis gas [4, 5] at high input energy as shown in Equation 1.



The synthesis gas (CO + H<sub>2</sub>) is converted to higher hydrocarbons or fuels via Fischer-Tropsch (FT) synthesis. The catalysts employed are based mainly on cobalt and iron at pressures as high as 22 bars and temperatures of higher than 560 K [6, 7].

A direct method for the conversion of methane includes the partial oxidation of methane to methanol [8, 9] or the oxidative coupling of methane (OCM) to C<sub>2</sub> hydrocarbons. In the oxidative coupling reaction, CH<sub>4</sub> and O<sub>2</sub> react over a catalyst at temperatures higher than 700 °C to form C<sub>2</sub>H<sub>6</sub>, C<sub>2</sub>H<sub>4</sub>, and CO<sub>2</sub>. Unfortunately, both the C<sub>2</sub>H<sub>6</sub> and the C<sub>2</sub>H<sub>4</sub> may be converted to CO<sub>2</sub>, and the single-pass combined yield of C<sub>2</sub>H<sub>4</sub> and C<sub>2</sub>H<sub>6</sub> (C<sub>2</sub> products) is limited to about 25% [1]. Over better catalysts, including SrO/La<sub>2</sub>O<sub>3</sub> [10] and Mn/Na<sub>2</sub>WO<sub>4</sub>/SiO<sub>2</sub> [11], a C<sub>2</sub> selectivity of about 80% can be achieved at a methane conversion of 20%. About half of the C<sub>2</sub> hydrocarbons obtained is C<sub>2</sub>H<sub>4</sub> and the rest is C<sub>2</sub>H<sub>6</sub>, although the C<sub>2</sub>H<sub>4</sub>/C<sub>2</sub>H<sub>6</sub> ratio can be enhanced by using a second catalyst. A high C<sub>2</sub> selectivity is almost always achieved under oxygen limiting conditions; thus the specific activity of the catalyst is not a factor. Because the overall reaction is exothermic, a zone within the catalyst bed may be 150-300 °C hotter than the external temperature [12]. Heat management in this process, therefore, is a serious engineering problem.

All the mentioned reactions need high intensive

energy input to establish high temperature or pressure.

To reduce energy costs, it is possible to use electric power in a plasma process instead of thermal processing. In most of gas discharge plasma, free molecular radicals generated by excitation, dissociation, and the ionization of gas molecules are essential for the subsequent free radical reactions. The control of electron energy by the suitable design of discharge reactor and the mode of gas discharge may lead to favorable products. Non-thermal plasmas at ambient temperature and pressure are recently being investigated as the promising alternative to convert methane to C<sub>2</sub> hydrocarbons [13-22]. Corona discharge, in which the geometry of electrodes is quite different like a needle and plate electrodes, is widely used for CH<sub>4</sub> conversion on laboratory scale [14-17]. Dielectric barrier discharge (DBD) is the most common used method of atmospheric pressure non-thermal plasma to convert methane to mainly oxygenate and methanol [17-21]. Recently pulsed power supplies of nanosecond rise time of voltage and current have been employed to improve the energy efficiency of plasma techniques for methane conversion [22-24].

The relative advantages of plasma techniques over conventional routes for the production of more valued products from methane is that, in gas discharge plasma, the main electrical energy is transferred to energetic electrons and active radical species rather than simple gas heating. As electrons process minor mass compared to heavy ions, they gain much higher speed in an electric field, and thereby a higher temperature. The electrons in a gas discharge collide with gas molecules and impart the whole or a portion of their kinetic energy to exit the molecules to a higher energy states. Ultimately, the molecule of the gas dissociates to radicals and other species and gives rise to the synthesis of new products [13].

In this study, methane conversion using atmospheric corona discharge was carried out in two parallel circular discs and different OCM catalyst prepared by impregnation method were investigated. The effect of input power, feed flow rate, and catalysts on the methane and oxygen conversion, the selectivity of products, and the yield of C<sub>2</sub> hydrocarbons were also studied.

## Experiments

The experimental set-up is shown in Figure 1. The corona discharge is maintained in the gap between a tungsten wire electrode with a thickness of 2 mm and a circular stainless steel disc with a diameter of 6.6 mm. The electrodes were housed in a quartz tube with an outer diameter (O.D.) of 7 mm and a wall thickness of 0.2 mm. A few holes were drilled in the circular electrode to allow the passage of gases from the plasma zone. The circular electrode in all the experiments was kept at the potential of zero, i.e. it was grounded; the wire electrode had different positive potentials. The wire electrode was perpendicular to the circular plate electrode at the centre at a distance of 10 mm from the disc electrode. The triggering voltage for maintaining gas discharge was supplied with a

regulated DC power supply, which could supply voltages up to 15 KV. The measuring system was composed of high voltage probe (Tektronix P6015), an oscilloscope (Tektronix, TDS 2024B), a galvanometer, and a gas chromatograph (GC). The feed gases, namely methane (99.999%), argon (99.999%), and oxygen (99.99%), were introduced into the discharge system via three mass flow controllers (Brooks, model 5850 TR).

The feed gases were mixed before entering the reactor by a static mixture, which was a 20 cm long stainless steel tube with a diameter of 3 cm filled with glass spheres. The feed gases (methane, oxygen, and argon) and the products were analyzed by an online gas chromatograph (Agilent 6890N) equipped with a flame ionization detector (FID) linked to alumina plot column and a thermal conductivity detector (TCD). This thermal detector was connected to HYSEP Q and N and molecular sieve 139 (MS-139) packed columns. The column temperature was programmable between 60 and 120 °C and the carrier gas was He and N<sub>2</sub>. The flow rate of carrier gas was 25 ml/min. At higher input power applied to the reactor, there were some liquid products collected in condenser, which were kept away without analysis.

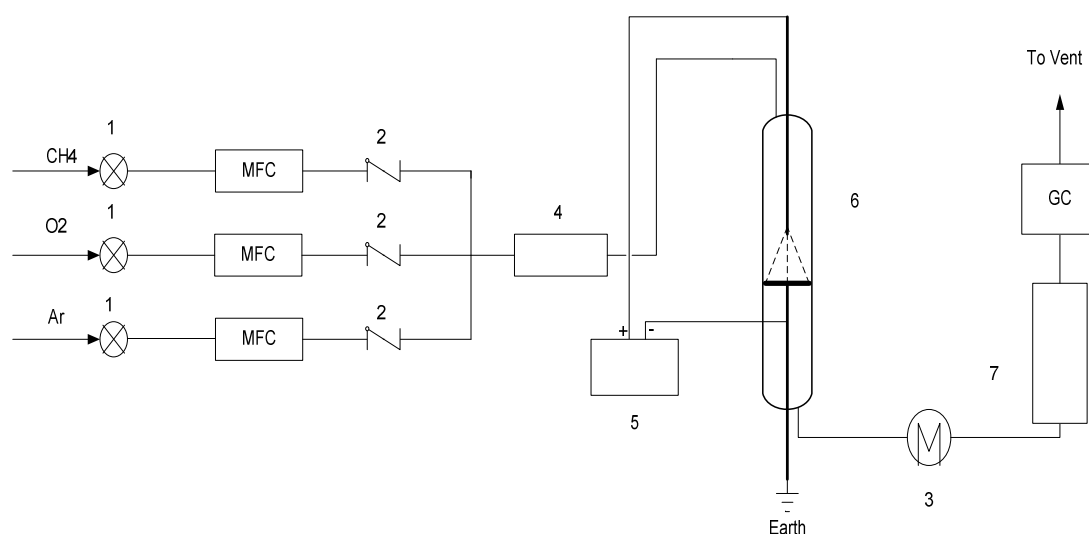


**Figure 1:** A schematic diagram of corona discharge reactor setup; (1) pressure regulator, (2) check valves, (3) condenser, (4) static mixer, (5) power supply, (6) reactor, and (7) silica gel.

## Catalyst Preparation

The first catalyst was prepared by sol-gel procedures; first pure sodium silicate solution (Merck) with a pH of 11-11.5 and 98% sulfuric acid (Merck) were slowly added together. The resulting solution was stirred at 80 °C for 2 hours until a pH of 8±0.1 was achieved. When the precipitation was completed, the obtained gel was filtered out, washed with warm de-ionized water, and dried at 120 °C followed by calcinations in air at 550 °C for 4 hours. The active components Na<sub>2</sub>WO<sub>4</sub> (5 wt.%) and Mn<sub>2</sub>O<sub>3</sub> (2 wt.%) was loaded to SiO<sub>2</sub> support by an incipient wetness impregnations procedure. The salts Mn(NO<sub>3</sub>)<sub>2</sub>·4H<sub>2</sub>O (Merck) 98.5% and Na<sub>2</sub>WO<sub>4</sub>·2H<sub>2</sub>O (Merck) 99% were dissolved in water, the amorphous SiO<sub>2</sub> precursor was gradually added to the solution, and the sample was dried by a rotary evaporator at 80 °C. The sample was dried at 120 °C overnight and calcined up to 800 °C for 16 hours under a flow of air at a heating rate of 3 °C per minute. The resulting powder catalyst Na<sub>2</sub>WO<sub>4</sub>/Mn<sub>2</sub>O<sub>3</sub>/SiO<sub>2</sub> were mixed thoroughly, pressed into tablets, crushed, and sieved to 20-40 mesh before use.

To investigate the effect of different sources on the catalyst precursor, tetraethyl orthosilicate (TEOS) 99.999% (Sigma Aldrich) was used as the SiO<sub>2</sub> source. 0.11 mol of tetraethyl orthosilicate was diluted with a molar ratio of 1:1 with ethanol, while stirring with a magnetic heater; 1.000 gr of multi-walled carbon nanotubes (CNT) (RIPI) was added to the solution; the resulted suspension was well mixed at 80 °C for 2 hours. In next step, water was removed from the suspension with a rotary evaporator at low pressure followed by drying the sample at 120 °C overnight. The active metals, i.e. manganese and tungsten, were supported on SiO<sub>2</sub> support taking the same procedure as for catalyst b1. The water was removed from the bulk in a low pressure rotary evaporator, dried at 120 °C and the sample was calcined at 850 °C in a flow of oxygen for 16

hours consequently the CNT was removed from the sample in the form of CO<sub>2</sub>. The solid obtained Na<sub>2</sub>WO<sub>4</sub>/Mn<sub>2</sub>O<sub>3</sub>/SiO<sub>2</sub>/ (TEOS) was designated as catalyst b2.

## Catalysts Characterization

Standard BET method was used to measure the specific surface areas of the prepared catalyst. The calculated values are shown in Table 1.

**Table1: Results of specific surface area of different supported catalysts**

Unit cell composition	Specific surface area (m <sup>2</sup> /gr)
SiO <sub>2</sub>	155
Na <sub>2</sub> WO <sub>4</sub> /Mn <sub>2</sub> O <sub>3</sub> / SiO <sub>2</sub> -b1	6
Na <sub>2</sub> WO <sub>4</sub> /Mn <sub>2</sub> O <sub>3</sub> / SiO <sub>2</sub> (TEOS)-b2	2
Na <sub>2</sub> WO <sub>4</sub> /Mn <sub>2</sub> O <sub>3</sub> /CNT- b3	110

The X-ray diffraction patterns of the catalysts were obtained by Philips PW 1840 diffractometer using Cu-Kα radiation. As it is clear from Figure 2, the XRD patterns of the SiO<sub>2</sub> as the support of the prepared catalysts investigated in this study show no specific line intensity, which indicates that it is an amorphous material. By supporting the active elements of Mn/W on the supports and subsequent calcinations at high temperatures, the resultant solid catalyst demonstrates a crystalline structure and exhibits the characteristic of α-cristoballite phase. Figure 3 shows the XRD patterns of the catalyst Na<sub>2</sub>WO<sub>4</sub>/Mn<sub>2</sub>O<sub>3</sub>/SiO<sub>2</sub>-b1, when active metals Mn/W are supported on the amorphous SiO<sub>2</sub> support and subsequently calcined at 850 °C. The two catalysts Na<sub>2</sub>WO<sub>4</sub>/Mn<sub>2</sub>O<sub>3</sub>/SiO<sub>2</sub> (TEOS)-b2 and Na<sub>2</sub>WO<sub>4</sub>/Mn<sub>2</sub>O<sub>3</sub>/CNT-b3 also show XRD patterns closely resembling Figure 3, but with weaker characteristic line intensities, which implies possessing lower crystallinity.

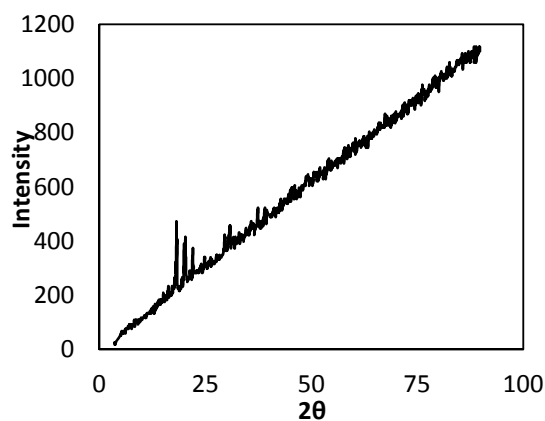


**Figure 2:** XRD patterns of SiO<sub>2</sub> prepared with sol- gel method

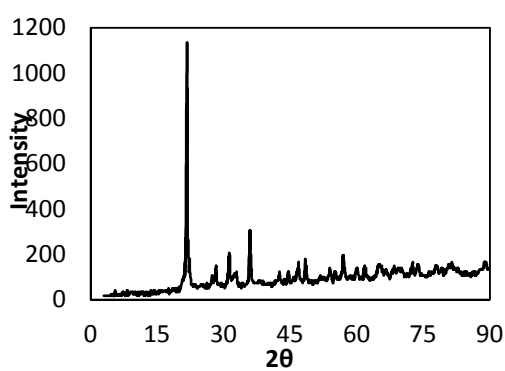


**Figure 3:** XRD patterns of Mn<sub>2</sub>O<sub>3</sub>/Na<sub>2</sub>WO<sub>4</sub>/SiO<sub>2</sub>-b1

## RESULTS AND DISCUSSION

The following relations were used to determine the conversion of reactant, selectivity and the yield of products.

$$\text{CH}_4 \text{ conversion} = (\text{moles of CH}_4 \text{ consumed} / \text{moles of CH}_4 \text{ introduced}) \times 100$$

$$\text{O}_2 \text{ conversion} = (\text{moles of O}_2 \text{ consumed} / \text{moles of O}_2 \text{ introduced}) \times 100$$

$$\text{Selectivity of C}_2\text{H}_6 = 2 \times (\text{moles of C}_2\text{H}_6 \text{ formed} / \text{moles of CH}_4 \text{ consumed}) \times 100$$

$$\text{Selectivity of C}_2\text{H}_4 = 2 \times (\text{moles of C}_2\text{H}_4 \text{ formed} / \text{moles of CH}_4 \text{ consumed}) \times 100$$

$$\text{Selectivity of C}_2\text{H}_2 = 2 \times (\text{moles of C}_2\text{H}_2 \text{ formed} / \text{moles of CH}_4 \text{ consumed}) \times 100$$

$$\text{Yields of C}_2 \text{ hydrocarbons} = \text{CH}_4 \text{ conversion} \times \sum (\text{Selectivity's of C}_2\text{H}_6, \text{C}_2\text{H}_4, \text{C}_2\text{H}_2)$$

## Effect of Input Power

All the experiments were carried out at atmospheric pressure and no external heating was used to heat the reactor. The first set of experiments were conducted using a corona discharge plasma at various feed flow rates and a fixed methane to oxygen ratio of 4:1 (volume basis). To enhance the stability of gas discharge, the feed was diluted with argon (60% of volume).

The effect of the input power and the total feed flow rates on methane and oxygen conversion is illustrated in Figure 4. The conversions of methane and oxygen are increased at higher levels of input power to the reactor. Increasing the input power to the reactor gives rise to an enhancement in the intensity of the internal electric field developed across the discharge gap; consequently, the density of high energy electrons in the generated gas discharge plasma will also increase. The high energy electrons upon interactions with methane and oxygen molecules will increase the probability of breaking the bonds between hydrogen and carbon in methane molecules and hence the methane conversion increases at higher levels of input power supplied to the reactor. Figure 4 also confirms that increasing the total flow rates to the reactor reduces the conversion of both methane and oxygen. It can be inferred that the energy levels of the electrons produced in gas discharge plasma are not equal but obey the Boltzmann's energy distribution function; hence only a limited number of electrons which have sufficiently high energy can participate in the formation of active species on collision with methane or oxygen molecules. When the residence time of the reaction decreases, the probability that each methane or oxygen molecule will successfully interact with any of the sufficiently high energy electrons is decreased, and thereby reducing the rate of methane and oxygen conversion.

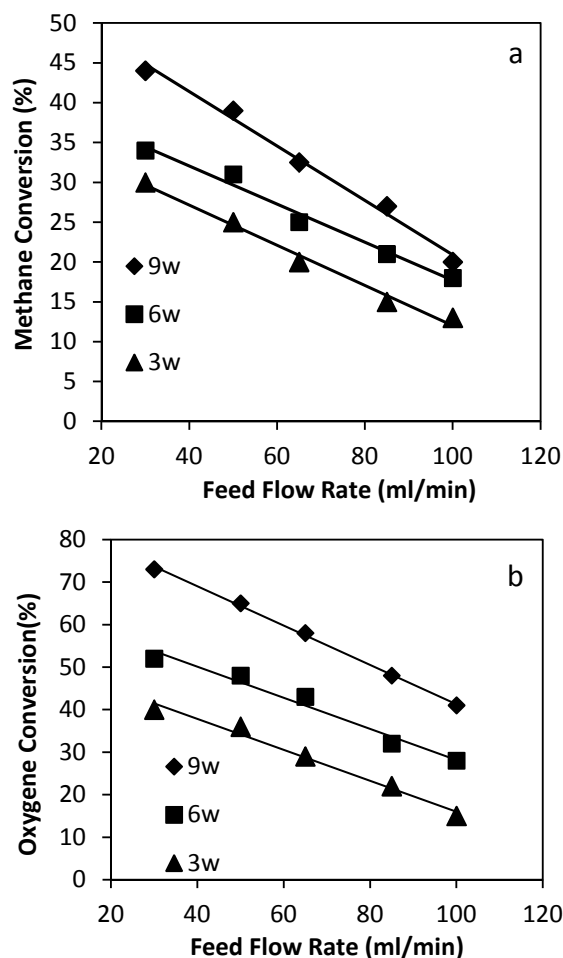


**Figure 4:** Effect of feed flow rates on conversion of methane and oxygen at various input powers to the reactor;  $\text{CH}_4/\text{O}_2$  ratio: 4:1; a) methane conversion and b) oxygen conversion.

The distribution of product selectivities at various input powers to the reactor and a fixed flow rate of 65 ml/min is shown in Figure 5. The formation of acetylene below 400°C at an ordinary temperature in plasma environment is very interesting, as its formation does not takes place in OCM reactions, which usually occur at temperatures above 600 °C. Carbon dioxide was not detected in these series of experiments at the measured temperatures up to 222 °C, which is not favorable for the formation of this gas. At higher levels of input power to the reactor, a fraction of higher hydrocarbon molecules dissociates to their radical spices and hence the selectivities of  $\text{C}_2$  products decreases, while the selectivity of carbon monoxide is increased. As the bond dissociation energy of

carbon monoxide is relatively high [26], at a higher field intensity, it remains stable and therefore its selectivity is improved.

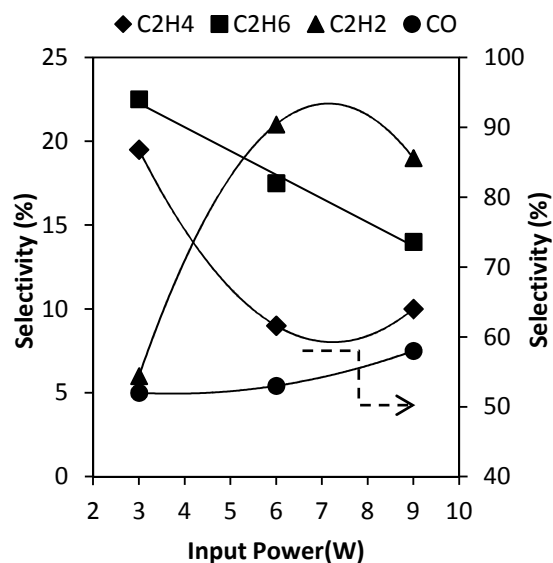


**Figure 5:** Selectivity of products vs. input power to the reactor;  $\text{CH}_4/\text{O}_2$  ratio: 4:1, flow rate: 65 ml/min, and input power: 3 W.

### Effect of Catalyst

To investigate the effect of the prepared catalysts on methane and oxygen conversion and product selectivities, 250 mg of the catalyst was introduced in the gap between the two electrodes. After each experiment, the tested catalyst was removed from the reactor, the reactor was cleaned, and finally fresh catalyst was loaded. To minimize the rate of coke formation, the new series of experiments was performed at an applied power of 3 Watt. Figure 6 demonstrates the methane and oxygen conversions at various feed flow rates to the reactor. The highest methane conversion (43%) belongs to the  $\text{Na}_2\text{WO}_4/\text{Mn}_2\text{O}_3/\text{SiO}_2$  (TEOS) catalyst. The catalyst  $\text{Na}_2\text{WO}_4/\text{Mn}_2\text{O}_3/\text{CNT-b3}$  in plasma environment has improved the  $\text{CH}_4$  conversion from 30%, when only gas discharge was available to 37%. The catalyst  $\text{Na}_2\text{WO}_4/\text{Mn}_2\text{O}_3/\text{SiO}_2$ -b1, however, demonstrates a slight raise in methane conversion; on the other hand, oxygen conversion shows a considerable enhancement.

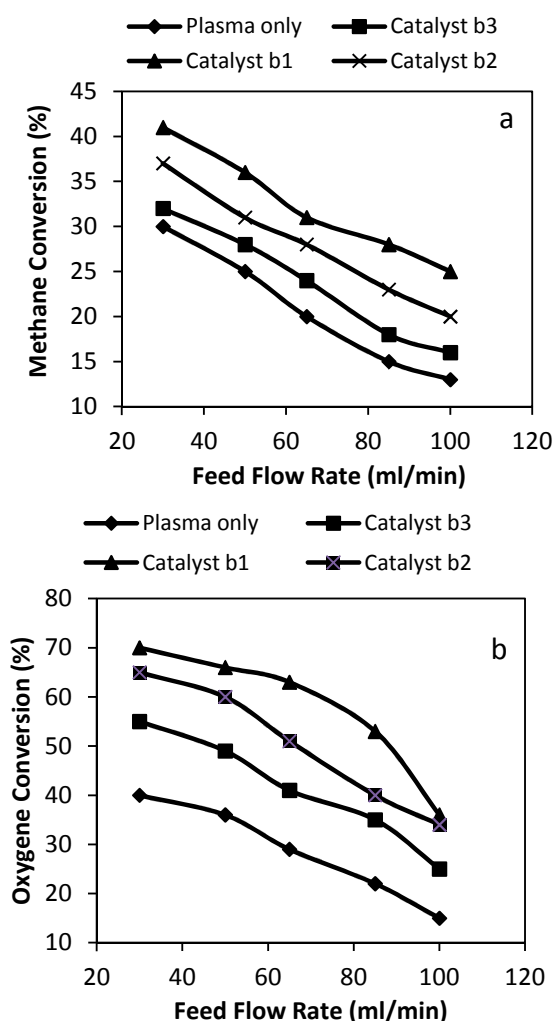


**Figure 6: Effect of feed flow rates on conversion of feed constituents in corona discharge plasma and over the catalysts b1, b2, and b3. Total flow rate: 65 cm<sup>3</sup>/min, CH<sub>4</sub>/O<sub>2</sub> ratio: 4:1, input power: 3W; a) methane conversion and b) oxygen conversion.**

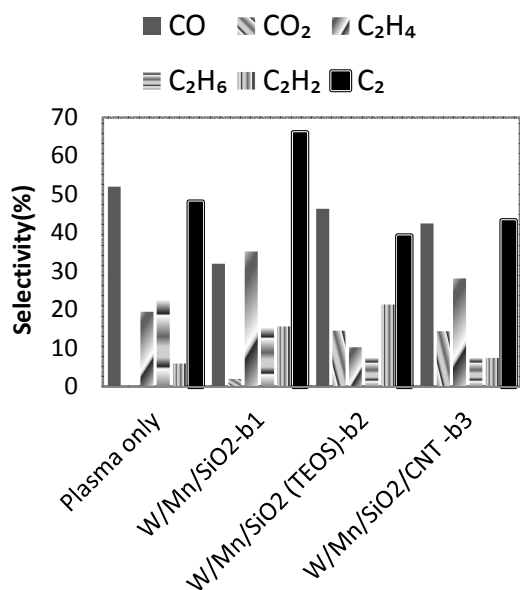
Figure 6 also demonstrates that by increasing the feed flow rates to the reactor the total conversion for oxygen and methane generally decreases. The rate of oxygen conversion in the combined plasma-catalyst system shows a high conversion at shorter residence times. For instance, when the catalyst b2 is present in plasma environment, it shows oxygen conversion up to 70%, while it is 40% in the absence of this catalyst.

Figure 7 demonstrates the changes in the selectivity of products at a fixed input power of 3 Watt and a total feed flow rate to the reactor of 65 ml/min. The formation of acetylene at the

measured temperature of up to 225 °C in a new set of experiments is an important phenomenon. All the three catalysts have increased the selectivity of ethylene. The stable gas discharge effect was observed over Na<sub>2</sub>WO<sub>4</sub>/Mn<sub>2</sub>O<sub>3</sub>/SiO<sub>2</sub>- (b1) and the process of coke formation was considerably delayed. For this reason, this catalyst is preferred to the other tested catalysts as it reduces the charges of maintenance and need for the frequent overhaul of large scale industrial units. The catalyst b1 also reduces the rate of formation of carbon monoxide and at the same time the selectivity to C<sub>2</sub> hydrocarbons is the highest compared to the other tested catalysts and gas discharge alone. The selectivity of the products over Na<sub>2</sub>WO<sub>4</sub>/Mn<sub>2</sub>O<sub>3</sub>/SiO<sub>2</sub> (TEOS)-b2 is interesting; this catalyst exhibits a high selectivity of carbon dioxide formations in OCM reactions in the temperature range of 770-850 °C. In the same way, this catalyst also shows a high carbon dioxide selectivity of about 15% in the plasma environment, which happens at a much lower temperature than its OCM reactions. Therefore, the overall effect of high CO<sub>x</sub> selectivity is a reduction in the selectivity of C<sub>2</sub> hydrocarbons. This catalyst also shows the highest acetylene selectivity.

In the presence of Na<sub>2</sub>WO<sub>4</sub>/Mn<sub>2</sub>O<sub>3</sub>/CNT- b3 catalyst, ethylene selectivity improves in plasma environment.

Figure 8 also compares the total yield of C<sub>2</sub>H<sub>4</sub> and C<sub>2</sub> hydrocarbons in discharge plasma environment, plasma combined catalysts at the measured temperature of 300 °C, and OCM reaction over b1 and b2 catalysts at 825 °C. The b3 catalyst was not tested in high-temperature OCM reaction, as it would eventually destroy and oxidize to carbon dioxide. Moreover, Figure 8 shows that the yield of ethylene is increased from 3.9%, when only plasma is the forcing agent, to 8.4%, when catalyst b1 is also available in discharge zone. The other two catalysts also show significance gain in the yield of C<sub>2</sub> hydrocarbons in plasma environment.



**Figure 7: Product selectivity of corona discharge plasma over the catalysts b1, b2, and b3; total flow rate: 65 cm<sup>3</sup>/min; CH<sub>4</sub>/O<sub>2</sub> mole ratio: 4:1; input power: 3W.**

Although the methane conversion in the combined plasma-catalytic conversion over this catalyst was higher than their corresponding OCM reactions, due to their high selectivity to carbon monoxide, their yield to higher hydrocarbons is still lower than their corresponding OCM reactions. According to Figure 8, the thermal catalytic methane conversions over catalyst b1 are 21.8% and 14% for C<sub>2</sub> hydrocarbons and ethylene yield respectively, while they are respectively reduced to 15.8% and 8.4% for the same catalyst in plasma environment.

An important point about W/Mn catalysts is that the catalysts show no sign of catalytic activity for methane conversion at temperatures below 650 °C. The enhancement of C<sub>2</sub> productions when they are placed in plasma environment indicates that there is a strong interaction between the free electrons of plasma and the active site of the three tested catalysts.

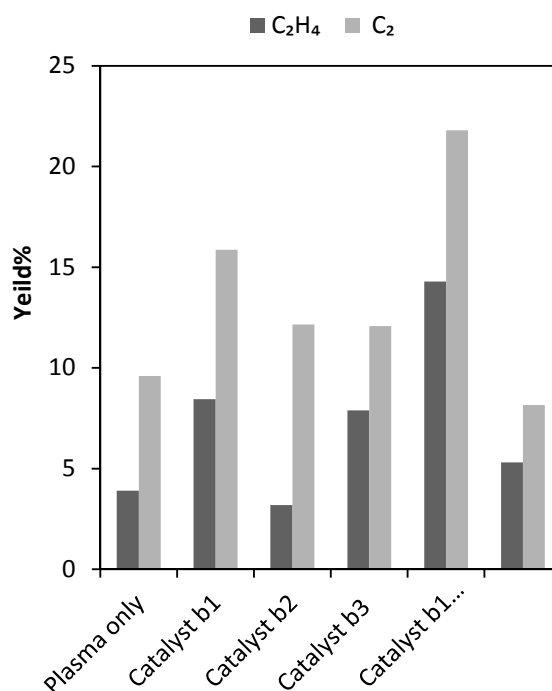


**Figure 8: The yield of hydrocarbons (ethylene and C<sub>2</sub>) in different conditions; total flow rate: 65 cm<sup>3</sup>/min; CH<sub>4</sub>/O<sub>2</sub> mole ratio: 4:1; input power: 3W.**

## CONCLUSIONS

The experimental investigations revealed that the direct formation of higher hydrocarbons from CH<sub>4</sub> could be demonstrated in a catalytic and non-catalytic DC corona discharge. The two catalysts, namely Na<sub>2</sub>WO<sub>4</sub>/Mn<sub>2</sub>O<sub>3</sub>/SiO<sub>2</sub> -b1 and Na<sub>2</sub>WO<sub>4</sub>/Mn<sub>2</sub>O<sub>3</sub>/SiO<sub>2</sub>/TEOS-b2, which were mainly used in OCM reactions, and the catalyst Na<sub>2</sub>WO<sub>4</sub>/Mn<sub>2</sub>O<sub>3</sub>/CNT-b3 enhanced the CH<sub>4</sub> conversion combined with gas discharge compared with gas discharge in the absence of catalysts. It was shown that the catalysts tested in the presence of gas discharge plasma improved the total yield to C<sub>2</sub> hydrocarbons. The catalyst Na<sub>2</sub>WO<sub>4</sub>/Mn<sub>2</sub>O<sub>3</sub>/SiO<sub>2</sub> -b1, which produced the least carbon oxides, gave rise to the highest productions of higher hydrocarbons and ethylene. The catalysts Na<sub>2</sub>WO<sub>4</sub>/Mn<sub>2</sub>O<sub>3</sub>/SiO<sub>2</sub>/TEOS-b2 and Na<sub>2</sub>WO<sub>4</sub>/Mn<sub>2</sub>O<sub>3</sub>/CNT-b3, due to their high selectivity toward carbon oxides, did not yield more valuable hydrocarbons. The catalyst b3 was



different from the other catalysts in the sense that the support of the catalyst b3 was multi-walled carbon nanotubes, which was electrically conductive. This catalyst conducted the corona discharge current and the overall discharge effect was the formation of a stable corona induced plasma and the inhibition of the formation of cokes. The ratio of yield of  $C_2H_4$  to  $C_2H_6$  for this catalyst was 3.7, which was the highest value compared to 2.3 and 1.3 for b1 and b2 catalysts respectively.

## ACKNOWLEDGEMENTS

The financial support by the Research and Technology Directorate of NIOC and the provision of the experimental facilities by Research Institute of Petroleum Industry (RIPI) are gratefully acknowledged.

## REFERENCE

- [1] Lunsford J. H., "Catalytic Conversion of Methane to More Useful Chemicals and Fuels," *Catal. Today*, **2000**, *63*, 165-173.
- [2] Holeman A., Olsvik O., and Rosktad O. A., "Pyrolysis of Natural Gas: Chemistry and Process Concepts," *Fuel Processing Technology*, **1995**, *42*, 249-260.
- [3] Serrano D. P., Botas J. A., and Guil-Lopez R., "H<sub>2</sub> Production from Methane Pyrolysis over Commercial Carbon Catalysts Kinetic and Deactivation Study," *International Journal of Hydrogen Energy*, **2009**, *34*, 44-88.
- [4] Holeman A., "Direct Conversion of Methane to Fuels and Chemicals," *Catal. Today*, **2009**, *142*, 2-8.
- [5] Rostrup-Nielsen J., "Production of Synthesis Gas," *Catalysis Today*, **1993**, *18*, 305-324.
- [6] Schulz H., "Short History and Present Trends of Fischer-Tropsch Synthesis," *Applied Catalysis A*, **1999**, *186*, 3-12.
- [7] Nakhaei Pour A., Housaindokht M. A., Tayyari S F., Zarkesh J. et al., "Deactivation Studies of Fischer-Tropsch Synthesis on Nanostructured Iron Catalyst," *Journal of Molecular Catalysis A*, **2010**, *330*, 112-120.
- [8] Qijian Z., Dehua H., and Qiming Z., "Direct Conversion of Methane into Oxygenates Role of Catalyst Location," *Natural Gas Chemistry*, **2008**, *17*, 24-28.
- [9] Otsuka K. and Wang Y., "Direct Conversion of Methane into Oxygenates," *Applied Catalysis A*, **2001**, *222*, 145-161.
- [10] Mimoun H., Robine A., Bonnaudet S., and Cameron C. J., "Recent Advances in the Oxidative Coupling of Methane," *Appl. Catal. A: Gen.*, **1990**, *58*, 269-280.
- [11] Fang X. and Li S., "Role of Sodium in the Oxidative Coupling of Methane over NA-W-MN/SiO<sub>2</sub> Catalysts," **1992**, 427.
- [12] Schweer D., Mleczko L., and Baerns M., "OCM in a Fixed-bed Reactor: Limits and Perspectives," *Catal. Today*, **1994**, *21*, 357-369.
- [13] Liu C., Marafee A., Hill B., Xu G., et al., "Oxidative Coupling of Methane with AC and DC Corona Discharges," *Ind. Eng. Chem. Res.*, **1996**, *35*, 3295-3301.
- [14] Liu C., Mallinson R., and Lobban L., "Hydrocarbons in a Corona Discharge over Metal Oxide Catalysts with OH Groups," *Applied Catalysis*, **1997**, *164*, 21-33.
- [15] Liu C., Mallinson R., and Lobban L., "Non-oxidative Methane Conversion to Acetylene over Zeolite in a Low Temperature Plasma," *Journal of Catalysis*, **1998**, *179*, 326-334.
- [16] Marafee A., Liu C., Xu G., Mallinson R. et al., "Methane Conversion to Higher Hydrocarbons in a Corona Discharge over Metal Oxide Catalysts with OH Groups," *Ind. Eng. Chem. Res.*, **1997**, *36*, 632.
- [17] Zhou L. M., Xue B., Kogelschatz U., and Eliasson B., "Partial Oxidation of Methane to Methanol with Oxygen or Air in a Non-equilibrium Discharge Plasma," *Plasma Chemistry and Plasma Processing*, **1998**, *18*, 375-393.
- [18] Liu Changjun., Mallinson R., and Lobban L., "Comparative Investigations on Plasma Catalytic Methane Conversion to Higher Hydrocarbons over Zeolites," *Applied Catalysis*, **1999**, *178*, 17-27.
- [19] Eliasson B., Jun Liu C., and Kogelschatz U., "Effect of Catalysts in Carbon Dioxide Reforming," *Ind. Eng. Chem. Res.*, **2000**, *39*, 1221-1227.

- [20] Aghamir F. M., Jalili A. H., Esfarayeni M. H., Khodaghali M. A. et al., "Conversion of Methane to Methanol in an AC Dielectric Barrier Discharge," *Plasma Sources Science and Technology*, **2004**, *13*, 707-711.
- [21] Haji Tarverdi M. S., Mortazavi Y., Khodadadi A. A., and Mohajerzadeh SH., "Conversion of Methane to C<sub>2+</sub> Hydrocarbons in a Dielectric Barrier Discharge Reactor," *Chemistry and Chemical Engineering*, **2005**, *24*(4), 63-71.
- [22] Yao S. L., Suzuki E., Meng N., and Nakayama A., "Effect of Voltage Waveform on Dielectric Barrier Discharge," *Energy and Fuels*, **2001**, *15*, 1300-1303.
- [23] Shuiliang Y., Suzuki E., and Nakayama A., "A Novel Pulsed Plasma for Chemical Conversion," *Thin Solid Films*, **2001**, *390*, 165-169.
- [24] Ghorbanzadeh A. M. and Matin N. S., "Methane Conversion to Hydrogen and Higher Hydrocarbons by Double Pulsed Glow Discharge," *Plasma Chemistry and Plasma Processing*, **2005**, *25*, 19-29.
- [25] Hongfei L., Yanying W., Jürgen C., and Haihui W., "Oxidative Coupling of Methane with High C<sub>2</sub> Yield by using Chlorinated Perovskite Ba<sub>0.5</sub>Sr<sub>0.5</sub>Fe<sub>0.2</sub>Co<sub>0.8</sub>O<sub>3-δ</sub> as Catalyst and N<sub>2</sub>O as Oxidant," *Chem. Cat. Chem.*, **2010**, *2*, 1539-1542.
- [26] Darwent B., "Bond Dissociation Energies in Simple Molecules," *U.S. National Bureau of Standards*, **1970**, 23.